Multi-Technique Characterisation of MOVPE-Grown GaAs on Si

C. S. Wong[1], N. S. Bennett[1], P. J. McNally[1], B. Galiana[2], P. Tejedor[2], M. Benedicto[2], J. M. Molina-Aldareguia[3], S. Monaghan[4], P. K. Hurley[4], K. Cherkaoui[4]

[1]*Nanomaterials Processing Laboratory, The Rince Institute, School of Electronic Engineering, Dublin City University, Dublin 9, Ireland.*

[2]*Instituto de Ciencia de Materiales de Madrid, C.S.I.C., Sor Juana Inés de la Cruz 3, 28049 Madrid, Spain*

[3]*IMDEA Materials, c/Professor Aranguren s/n, 28040 Madrid, Spain.*

[4]*Micro-Nanoelectronics Centre, Tyndall National Institute, University College Cork, Ireland*

The heterogeneous integration of III-V materials on a Si CMOS platform offers tremendous prospects for future high speed and low power logic applications. That said this integration generates immense scientific and technological challenges. In this work multi-technique characterisation is used to investigate properties of GaAs layers grown by Metal-Organic Vapour Phase Epitaxy (MOVPE) on Si substrates - (100) with 4° offset towards <110> - under various growth conditions. This being a crucial first step towards the production of III-V template layers with a relatively lower density of defects for selective epitaxial overgrowth of device quality material. The optical and structural properties of heteroepitaxial GaAs are first investigated by micro-Raman spectroscopy and photoluminescence and reflectance measurements. High-resolution X-ray diffraction (HR-XRD) is used to investigate structural properties. Advanced XRD techniques, including double-axis diffraction and X-ray crystallographic mapping are used to evaluate degrees of relaxation and distribution of the grain orientations in the epilayers, respectively. Results obtained from the different methodologies are compared in an attempt to understand growth kinetics of the materials system. The GaAs overlayer grown with annealing at 735°C following As predeposition at 500°C shows the best crystallinity. Close inspection confirms the growth of epitaxial GaAs preferentially oriented along (100) embedded in a highly-textured polycrystalline structure.

1. Introduction

Successful heterogeneous integration of III-V materials on Si is a target of the electronics industry since these compound semiconductors offer a solution to future high speed and low power logic applications [1-5]. GaAs is a desirable material for modern microelectronics due to properties that include a large band gap, high carrier mobility, stability against radiation, good response rate, and low energy losses in the devices and integrated circuits based upon it. Nevertheless, extensive use of GaAs substrates is prohibitively expensive. It is more cost-effective to deposit epitaxial layers of GaAs on a comparatively cheap substrate, such as Si, which is the industry substrate of choice.

Various key issues must be overcome for successful growth of high-quality GaAs on Si. Problems with anti-phase domains (APD) appearing in GaAs epilayers can be removed by

using either Ga or As pre-layers and tilted substrates [1,2] together with an optimized substrate preparation in order to get a clean double-step surface. Nevertheless, the key challenge lies in the significant 4.1% lattice mismatch and 63% thermal expansion mismatch between GaAs and Si. These factors mean abundant extended defect densities are generated in the epitaxial layers when the principal techniques – namely liquid phase epitaxy (LPE), molecular beam epitaxy (MBE), chemical beam epitaxy (CBE) and metal-organic vapour phase epitaxy (MOVPE) – are employed. The selection of appropriate growth conditions (growth/annealing temperatures, Ga/As flux ratios and layer thickness) is an essential first step towards production of template layers with a relatively lower density of defects for selective epitaxial overgrowth of device quality material.

This work focuses on the complementary methods that can be used for characterisation of MOVPE-grown GaAs on Si under various substrate preparation conditions.

2. Experimental Details

GaAs/Si samples were grown by MOVPE in a 2" AIX200/4 horizontal reactor system. Si epi-ready (100) substrates, 350 μm in thickness and misoriented by 4^{o} towards the nearest (110) plane were used. The MOVPE growth process took place at a pressure of 100 mbar and with a total flow of 14 slpm of palladium-purified hydrogen, using precursors arsine (AsH_3) and tri-methyl-gallium (TMGa) precursors. The MOVPE routine consisted of these main steps: i) low temperature annealing at 500ºC in H_2 for 15 min, ii) Si substrate preparation by high temperature annealing in H_2 and/or annealing in AsH_3 (As monolayer deposition), iii) low-temperature deposition of a GaAs nucleation layer (T = 500ºC, V/III = 120) and iv) growth of a GaAs buffer layer (T = 640ºC, V/III = 55). Prior to epitaxy, three of the samples were cleaned in a VARIAN-360 MBE system using atomic hydrogen irradiation at a substrate temperature of 630 ºC at a background pressure of 10^{-6} torr for 45 min. Atomic hydrogen was generated by dissociation of H_2 gas at a W filament (1800ºC) in a home-built cracker cell working at an acceleration voltage of 2.5 kV and ionization currents in 30-35 mA range. Table I summarizes the growth routine employed for each sample. Each sample has been exposed to different growth conditions from sample to sample in order to identify significant effects of each process. The layer thickness listed in Table I are nominal values and some variation from these values are evident in preliminary thickness measurements.

The quality of the samples was investigated using a Jobin Yvon Horiba LabRAM 800 spectroscopic system with an Ar^{+} laser (λ = 488 nm), used to capture both the micro-Raman spectra and photoluminescence (PL) at room temperature. The laser was focused on the sample surface to a spot diameter of 1μm with an Olympus 100X microscope objective. An integration time of 10s was selected and three micro-Raman and PL spectra from the same probing position were averaged to increase the signal-to-noise ratio (SNR). All peaks were searched and fitted with Gaussian-Lorentzian functions using a computer program, which is provided by the data acquisition system of the Raman spectrophotometer.

In addition all samples were studied using a triple-axis Jordan Valley Bede-D1 X-ray diffractometer using a monochromatic Cu-Kα (λ = 1.5405Å) radiation source operated at 45kV and 40mA. Polycrystalline X-ray Diffraction (XRD) and high-resolution double-axis X-ray diffraction (HR-XRD) rocking curves (RCs) were used to analyze the crystallite structure of the GaAs overlayers. In order to eliminate the effects of tilt between the epilayer and substrate and the anisotropy of the elastic strain distribution, four pairs of (004) and (224) RCs were repeated by successive 90^o rotations of the sample around the [001] axis. The average angular peak separations were used in estimating the strain/relaxation of the GaAs layer. The measured HR-XRD RCs are modelled using JV-HRXRD software [6]

X-ray pole plots are employed to investigate the distribution of grain orientations. Each scan was run by setting the sample and detector angles together in a 2:1 ratio ($2\theta:\omega$). This allows different interplanar spacings to be measured for the same sample tilt – especially useful for samples with preferred orientations. A full X-ray pole figure is recorded by rotating the sample for a phi (Φ) range from 0^0 - 360^0 for each incremental value of the chi angle (χ: 0^0- 90^0).

3. Results and Discussion

Fig. 1 shows the micro-Raman spectra for each of the MOPVE-grown GaAs on Si samples (1) – (4). Raman spectra from these GaAs layers comprise of two intense crystalline GaAs Raman peaks corresponding to the transverse optical (TO) and longitudinal optical (LO) modes at 266 and 289 cm^{-1}, respectively. In each case the peak at 521cm^{-1} is characteristic of the optical vibration TO phonon mode from the mono-crystalline Si substrate. The variation of Si peak intensity is a signature of the thickness variation of the overlying GaAs film. Since the penetration depth of the λ=488 nm laser probe is ~ 90 nm in GaAs and ~ 570 nm in Si, a thicker GaAs layer results in a smaller volume of Si contributing to the Raman spectral signals.

In each case the GaAs LO and TO Raman peaks are red shifted by ~3 cm^{-1} compared with the peak position for bulk GaAs together with a peak full width at half maximum (FWHM) broadening of ~4cm^{-1}. This peak red shifting and broadening is an indication of defects generated within the GaAs films during the growth process [7]. These are due to the breaking of translational symmetry in the momentum selection rule for Raman scattering, wherein phonons in the first Brillouin zone with $q \neq 0$ contribute to the Raman spectra, thus lower frequency vibrations become Raman-active and dominate the spectrum [7,8].

Moreover, the spectra of these GaAs samples shows a broad peak centred at ~200cm^{-1} which is associated with As-cluster vibration modes [9-11]. Arsenic within the GaAs structure can contribute to the generation of As-As bonds and As-related point defects, such as As_{Ga} antisite defects and Ga vacancies [11]. These indirectly induce changes in the average reduced mass and effective ionic charge that further enhances the red shifting of the Raman peaks [11]. The precipitate peak is more intense for samples (1) and (2), suggesting a greater density of As precipitates in these samples compared to samples (3) and (4). However intensity variations due to differences in GaAs thickness from sample-to-sample cannot be

completely discounted. Among these GaAs/Si samples, sample (4) shows two sharp and intense peaks located at ~194cm^{-1} and ~257cm^{-1} that are ascribed to the E_g and A_{lg} Raman-active phonons of crystalline arsenic [8, 11]. These peaks are only significant in sample (4), presumably due to its longer As pre-deposition times.

With reference to Fig. 2, it is significant that sample (4) produces the highest PL intensity, being at least a factor of 2 greater than the other samples. This is a signature of improved crystal quality and is also consistent with the elimination of APD-related effects. Also sample (3) demonstrates some luminescence, and since the high temperature annealing process is unique to samples (3) and (4), it appears that this is contributory to the improved quality. Samples (1) and (2) show almost no luminescence in comparison. In sample (4) luminescence is centred on ~888.5nm, which is red shifted around 11nm with respect to bulk GaAs. The red shift is related to two factors. First, the biaxial compressive stress due to presence of excessive arsenic in the crystal – since the covalent radius of As (1.18Å) is smaller than that of Ga (1.28Å) and thus, compressive stress is generated [13]. In addition, the lattice mismatch between GaAs and Si will produce compressive stress in the GaAs overlayer.

Fig. 3 shows the 2θ-ω X-ray diffraction spectrum for MOVPE-grown sample (4). This powder diffraction scan for MOVPE-grown GaAs/Si shows evidence of polycrystallinity in the film. GaAs diffraction peaks of the (111), (220), (311) and (400) planes are labelled in Fig. 4. The average crystallite size in each sample is calculated from the FWHM of the (111) diffraction peak using the Scherrer formula [14]. A slight reduction in the calculated average lattice parameter for these GaAs materials reflects the presence of compressive stress as previously implied. Considering these results in parallel with growth parameters in Table I it would appear that larger crystallites are associated with longer annealing and pre-deposition times. Comparing samples (1) and (2) across Figs. 1 to 3, it appears that applying the *ex situ* H clean has relatively little impact on the quality of the grown GaAs layers. If anything, the sample not receiving cleaning (sample 1) is of better quality, possibly due to re-oxidation of the Si before pre-deposition. However considering sample (3), it is clear that a further annealing step at 735^{o}C (beyond the standard 500^{o}C anneal) increases the crystallite size and quality of the epitaxial GaAs. Increasing the As pre-deposition time further improves the crystallinity of GaAs layer (sample 4).

In HR-XRD measurements, a broad and weak intensity GaAs peak is consistently observed around $\Delta\omega \sim$ -8500 arc-sec in the (004) ω-2θ RC of all samples (1) – (5). This peak can be interpreted as being due to diffracted intensities from a mosaic, but highly textured, poly-crystalline GaAs structure, with each mosaic region contributing diffracted intensity throughout a particular angular range. However, the peak is not apparent in the (224) ω-2θ RC. This is expected since a highly textured polycrystalline film produces diffraction in the out-of-plane lattice parameter but is not in the in-plane direction [6, 15]. Fig. 4 shows both the (004) and (224) HR-XRD RCs of sample (4) and the corresponding Bede RADS structural simulations. The (004) RC shows an additional GaAs peak that is of interest, located at $\Delta\omega\sim$-5500 arc-sec. This peak corresponds to the GaAs peak located at $\Delta\omega \sim$ -8000 arc-sec in the (224) RC, which is diffracted from fully relaxed GaAs epitaxial material. The

shape of the GaAs peak in the (224) RC is asymmetric and thus can be associated with the presence of azimuthal anisotropy of the elastic strain distribution [16]. Detailed analysis of the (224) RC reveals that the GaAs epitaxial is in slightly compressive stress with 99% relaxation.

It can be noted that Pendellősung fringes are not significant in these RCs. If fringes are forbidden it is typically an indication of defective GaAs layers [16] due to the various issues encountered in heteroepitaxial growth of GaAs on Si.

Throughout this study sample (4) – subjected to an elongated As pre-deposition time – has demonstrated the most interesting features and thus we highlight its further characterisation using crystallographic mapping. Fig. 5 shows the <111> pole figure for sample (4) recorded using GaAs <111> diffraction angles at $2\theta = 27.38^{\circ}$. The <111> pole figure shows the four-fold symmetry peaks located at $\Psi = \sim 54.7^{\circ}$, which are attributed to epitaxial GaAs orientated to the (100) plane. An initial estimate suggests that up to 10% of GaAs takes this orientation. However, the peak widths in the pole density distribution are broadened showing that the alignment of the epitaxial grains is not perfect. This is thought to be the signature of misoriented GaAs grains. The misorientation could originate from crystal defects and dislocations generated during growth. Alternatively, the presence of arsenic precipitation-induced lattice strain might lead to the misorientation [17]. In this case, the crystallites tilt slightly to various directions due to mosaicity or misorientations within the crystal and the four-fold symmetry peaks are broadened. In other words, $\Delta\Psi$ directly reflects the tilt misorientation and $\Delta\Phi$ contains contributions from the tilt and rotational misorientations [18].

In addition, a 'ring' contour pattern is observed around the centre in the <111> pole figure. This is attributed to the diffracted intensity collected from highly textured polycrystalline material and it rotates with varying Φ around a centre axis parallel to the substrate normal along <111>. This reveals that, besides the aforementioned epitaxial material, there is some preferential polycrystalline grain orientated to <111>.

There are several peaks with weaker diffraction intensity at $\Psi = \sim 72^{0}$ (denoted as T_n in Fig. 5), in addition to the four-fold symmetry peaks of the epitaxial grains (labelled as A_n in Fig. 5). These could result from further epitaxial orientation associations between GaAs and Si. For example, it is well known that twins are commonly formed in zincblende III-V crystals by {111} planes rotating 60^{0} around <111>. This consequently leads to the existence of twinning angles $\theta_t = 38.94^{0}$ and 56.25^{0} between certain <111> lattice directions of the two twins [19, 20]. A detailed analysis shows that the orientations of the 8 weaker diffraction intensities denoted as (T_n, n = 1, 2, ... 8) are tilted at $\sim 35^{0}$ from the high symmetry point. These are within a few degrees of the expected orientations of the <111> poles of first order twins generated on epitaxially oriented grains.

4. Conclusions

Growth of GaAs on Si offers tremendous prospects for future high speed and low power logic applications. Successful growth is however non-trivial and comprehensive characterisation is key to identifying a successful way forward. GaAs/Si samples, like the template layers for selective epilayer overgrowth, were grown by MOVPE and characterised using micro-Raman spectroscopy, PL and HR-XRD techniques. Powder diffraction confirms poly-crystallinity in the MOVPE-grown GaAs layers. However, analysis of the experimental HR-XRD RCs reveals the existence of 99% relaxed epitaxial GaAs embedded in the highly-textured polycrystalline structure. Of particular interest, X-ray crystallographic mapping confirms the presence of up to 10% of epitaxial GaAs preferentially oriented along (100). Various growth parameters have been altered in growing GaAs on Si. It appears that employing an *ex-situ* H clean has relatively little impact on the quality of the grown GaAs layers. However it is clear that a further annealing step at 735^{o}C (beyond the standard 500^{o}C anneal) increases the crystallite size and quality of the epitaxial GaAs. Increasing the As pre-deposition time further improves the crystallinity of GaAs layer.

Acknowledgements

This work was supported by the EU FP7 MNT ERA-Net 'ENGAGE' project with local support from Enterprise Ireland and Fundación madrimasd para el Conocimiento. Financial support by MICINN under grant TEC2007-66955 is gratefully acknowledged, as are Dr. C. Algora and Dr. I. Rey-Stolle from the Solar Energy Institute of the Polytechnic University of Madrid for access to the MOVPE reactor.

References

[1] S. F. Fang, K. Adomi, S. Iyer, H. Morkoc, H. Zabel, C. Choi, N. Otsuka, J. Appl. Phys. 68 (1990) R31.

[2] S.F. Cheng, L. Gao, R. L. Woo, A. Pangan, G. Malouf, M. S. Goorsky, K. L. Wang, R. F. Hicks, J. Crystal Growth 310 (2008) 562.

[3] P. J. Taylor, W. A. Jesser, J. D. Benson, M. Martinka, J. H. Dinan, J. Bradshaw, M. Lara-Taysing, R. P. Leavitt, G. Simonis, W. Chang, W. W. Clark III, K. A. Bertness, J. Appl. Phys. 89 (2001) 4365.

[4] Y. Chang, T. H. Yang, G. Luo, C. Y. Chang, J. Elec. Mat. 34 (2005) 23.

[5] A. Ito, M. Ichimura, A. Usami, T. Wada, H. Kano, J. Appl. Phys. 72 (1992) 2531.

[6] See www.jvsemi.com

[7] S. W. Da Silva, D. I. Lubyshev, P. Basmaji, Yu. A. Pusep, P. S. Pizani, J. C. Galzerani, R. S. Katiyar, G. Morell, J. Appl. Phys. 82 (1997) 6247.

[8] K. K. Tiong, P. M. Amirtharaj, F. H. Pollak, D. E. Aspnes, Appl. Phys. Lett. 44 (1984) 122.

[9] R. R. Campomanes, J. Vilcarromero, J. C. Galzerani, J. H. Dias Da Silva, Appl. Phys. A, 80 (2005) 267.

[10] R. L. Farrow, R. K. Chang, S. Mroczkowski, Appl. Phys. Let. 31 (1997), 768.

[11] D. S. Jiang, X. P. Li, B. Q. Sun, H. X. Han, J. Phys. D: Appl. Phys. 32 (1999). 629.

[12] P. S. Pizani, A. Mlayah, J. Groenen, R. Carles and A. Claverie, Appl. Phys. Lett. 66 (1995) 1927.

[13] F. Zhang, H. Tu, Y. Wang, J. Qian, H. Wang, J. Wang, P. Song, Mater. Sci. Eng. B 75 (2000) 139.

[14] J. Nayak, S. N. Sahu, Appl. Sur. Sci. 182 (2001) 407.

[15] A. Lankienen et al, Crystal Growth and Design, 6 (2006) 1096.

[16] T. K. Sharma, S. D. Singh, S. Porwal, A. K. Nath, J. Cryst. Grwth. 298 (2007) 527.

[17] K. Balakrishnan, G. Feuillet, K. Ohta, H. Hamaguchi, H. Okumura, S. Yoshida, Jpn. J. Appl. Phys. 36 (1997) 6221.

[18] M. Schreck, B. Stritzker, Phys. Stat. Sol (a), 154 (1996) 197.

[19] J. B. Misiuk, E. Dynowska, A. Misiuk, M. Calamiotou, A. Kozanecki, J. Domagala, D. Kuristyn, W. Glukhanyuk, A. Georgakilas, J. Terala, J. Adamczewska, Cryst. Res. Tech. 36 (2001) 997.

[20] G. Brammertz, Y. Mols, S. Degroote, V. Motsnyi, M. Leys, G. Borghs, M. Caymax, J. Appl. Phys. 99 (2006) 3514.

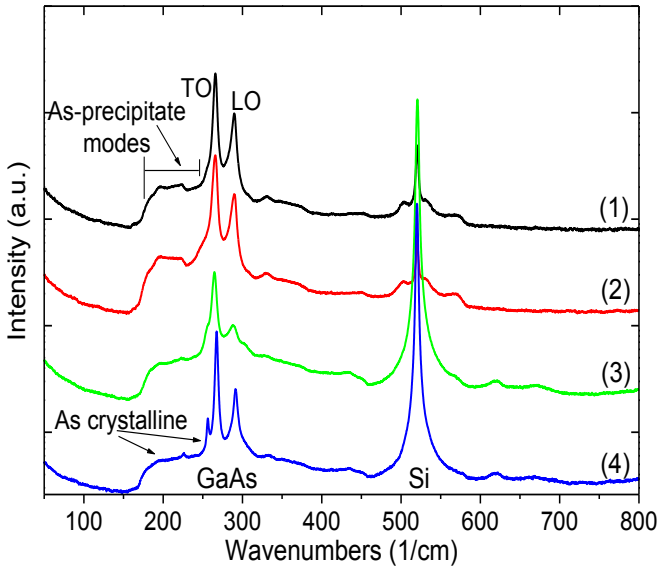

Figure 1. Room temperature Raman spectra for GaAs/Si samples (1)-(4).

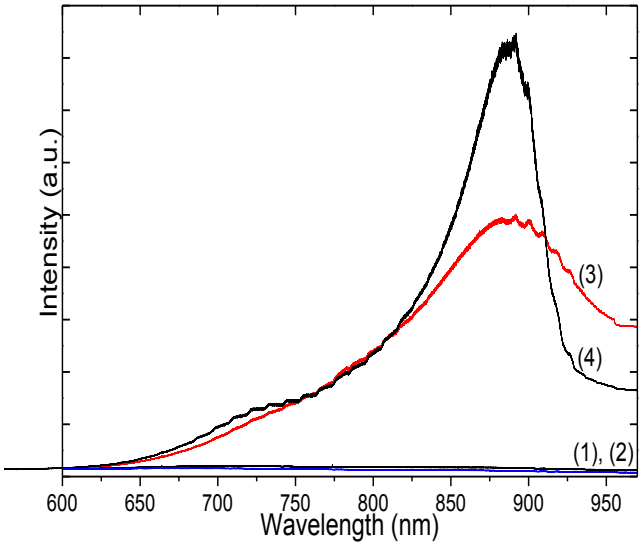

Figure 2. Room temperature photoluminescence spectra for GaAs/Si samples (1)-(4)

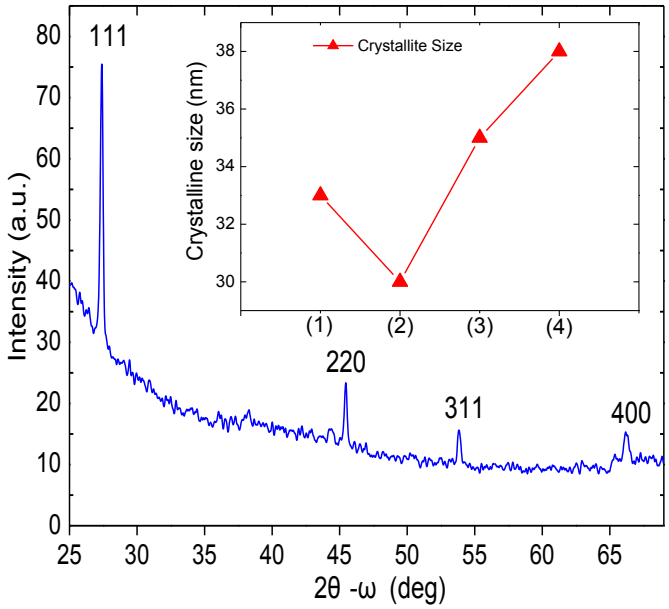

Figure 3. *2θ-ω* poly-crystalline XRD measurement for GaAs/Si sample (4). Inset shows average crystallite size in samples (1)-(4).

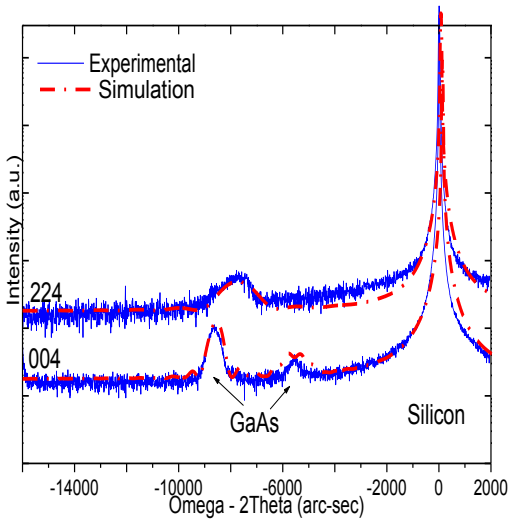

Figure 4. *θ-2ω* 004 and 224 HR-XRD RCs and corresponding simulations of MOVPE-grown GaAs/Si sample (4).

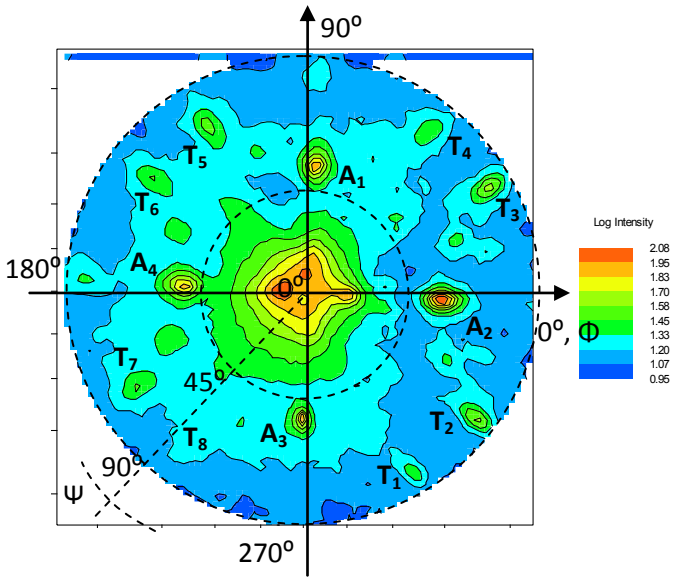

Figure 5. GaAs pole plot of sample (4) for (111) diffraction. Four-fold symmetry of GaAs epitaxial grains is denoted as A_n in the pole figure. T_n refers to diffraction corresponding to twin boundaries.

Table I. Growth details of MOVPE-grown GaAs/Si samples (1) – (4)

Sample	Ex-situ H cleaning	Low temp (500°C) annealing time (s)	High temp (735°C) annealing time (s)	As pre-deposition (500°C) time (s)	Low temp (500°C) GaAs buffer thickness (nm)	High temp (640°C) GaAs buffer thickness (nm)
1	No	900	-	150	60	200
2	Yes		-	150	60	200
3	Yes		900	150	60	200
4	Yes		900	900	180	-